

Introduction

Nova 018 is an ureilite which are magmatic, ultramafic achondrites composed of olivine and clinopyroxene (CPX), with interstitial carbonaceous material [1]. A unique characteristic of ureilites is the presence, and abundance (up to 3 wt%), of elemental carbon [2].

Ureilites are particularly interesting because carbon can appear as diamond. The method of formation and concentration of the carbon phases, however, remains unresolved [3]:

- high-pressure, high-temperature (HPHT) growth within the ureilite parent body (UPB) [4]
- low pressure chemical vapor deposition (CVD) [5]
- high-pressure shock from an impact event [6].

We have described and analyzed Nova 018 to contribute to known ureilite literature and have identified an opportunity to conduct further analysis into the meteorite's diamondiferous nature.

Figure 1: Photograph of the main fragment with mass of 1.79 kg. Dimensions are 13.0 x 9.5 x 10.4 cm. [7]



Methodology

Element maps and backscattered electron (BSE) images were acquired using a JEOL JXA-8320 Electron Probe Microanalyzer (EPMA), at the University of Toronto, Canada. Unknown phases were identified using a Horiba LabRAM Aramis micro-Raman spectrometer at the Royal Ontario Museum (ROM) by comparing results to the RRUFF database [8]. High-resolution cathodoluminescence (CL) images were acquired by a Hitachi SU6600 Scanning Electron Microscope (SEM) at Western University.

Observed Petrography

Total mass is 2.1 kg, spread across 13 fragments with the largest piece measuring 1.79 kg (**Figure 1**). Nova 018 exemplifies typical ureilite mineralogy and textures [9,10]:

- 70% Magnesium-rich forsterite.
- 27% Pigeonite.
- 3% interstitial carbonaceous material.
- Olivine exhibits planar fracturing and mosaicism indicating a shock stage of S4, or high-shock level [11,12].
- Significant reduction of silicates with varying widths of reduction rims, ranging from approximately 100 μm to nearly 2 mm.
- The rims surrounding forsterite grains contain many inequigranular metal inclusions, ranging from < 1 μm to 200 μm , and in some instances, contain carbon (**Figure 2**). The rims surrounding pigeonite cores are narrower and have fewer metal inclusions.

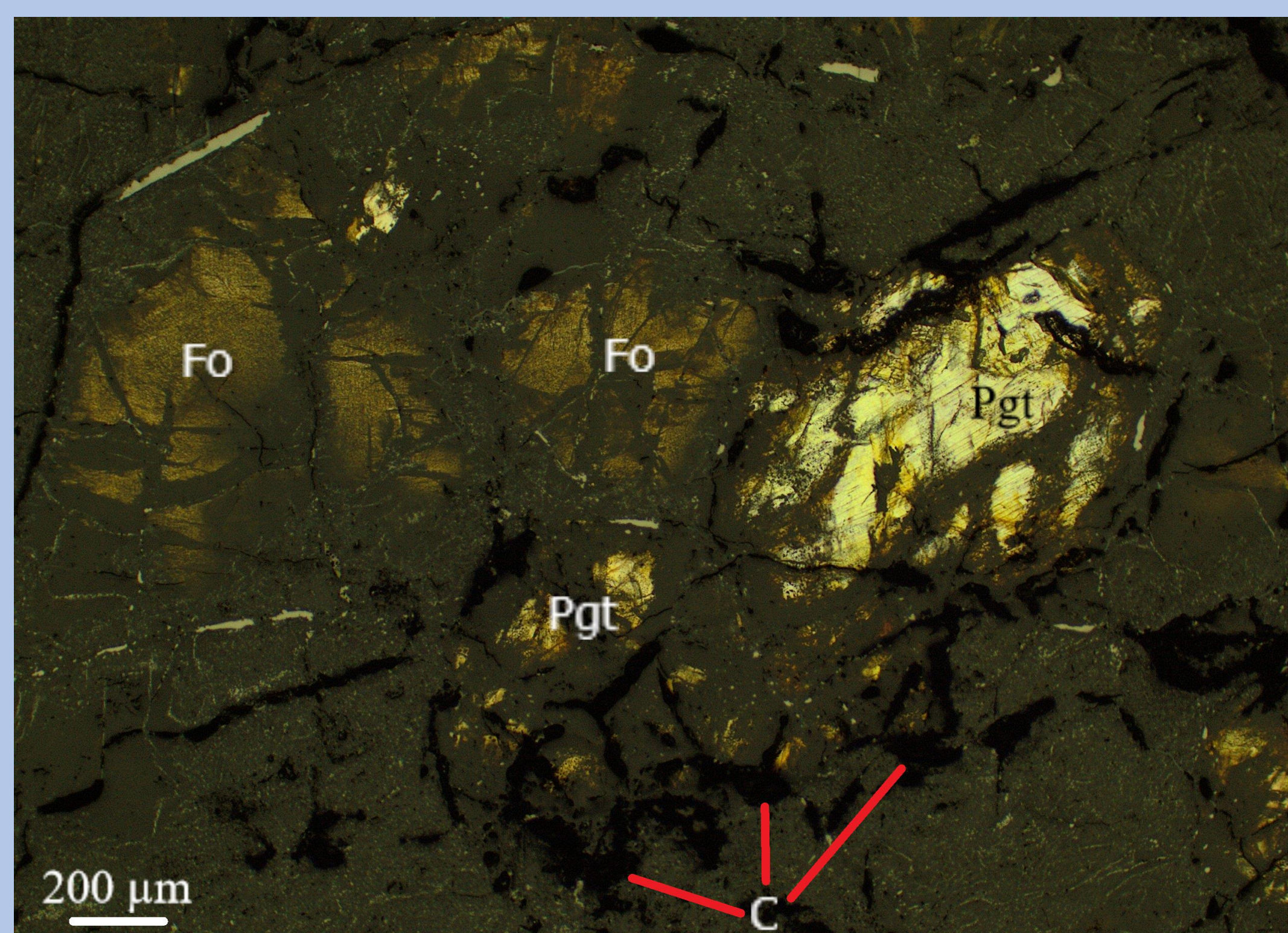


Figure 2: Photomicrograph in plane polarized and reflected light. Carbon (C) shows greater affinity to pigeonite (Pgt) than forsterite (Fo) and appears to have been injected into the former.

Carbonaceous Material

- Heterogeneously distributed.
- Found around or within pigeonite grains, where it appears as injections, and only appears within the reduction rims of olivine grains (**Figures 2, 3**).
- Appear as anhedral to bladed laths. Individual domains range up to 700 μm in diameter.

Images acquired by SEM-CL and BSE reveal highly diamondiferous phases dispersed among graphite and amorphous carbon phases.

- Using CL at low magnification, diamonds appear very bright yellow and blue spots (**Figure 5d**).
- The diamonds have variable dimensions, ranging from nanometer-sized upwards to 100 μm (**Figure 5**).
- Diamonds are found either as individual grains or within clusters (**Figures 5a, b**). Higher magnification BSE and color CL images reveal the structure and zonation of individual grains and diamond clusters (Figure 4c, d).

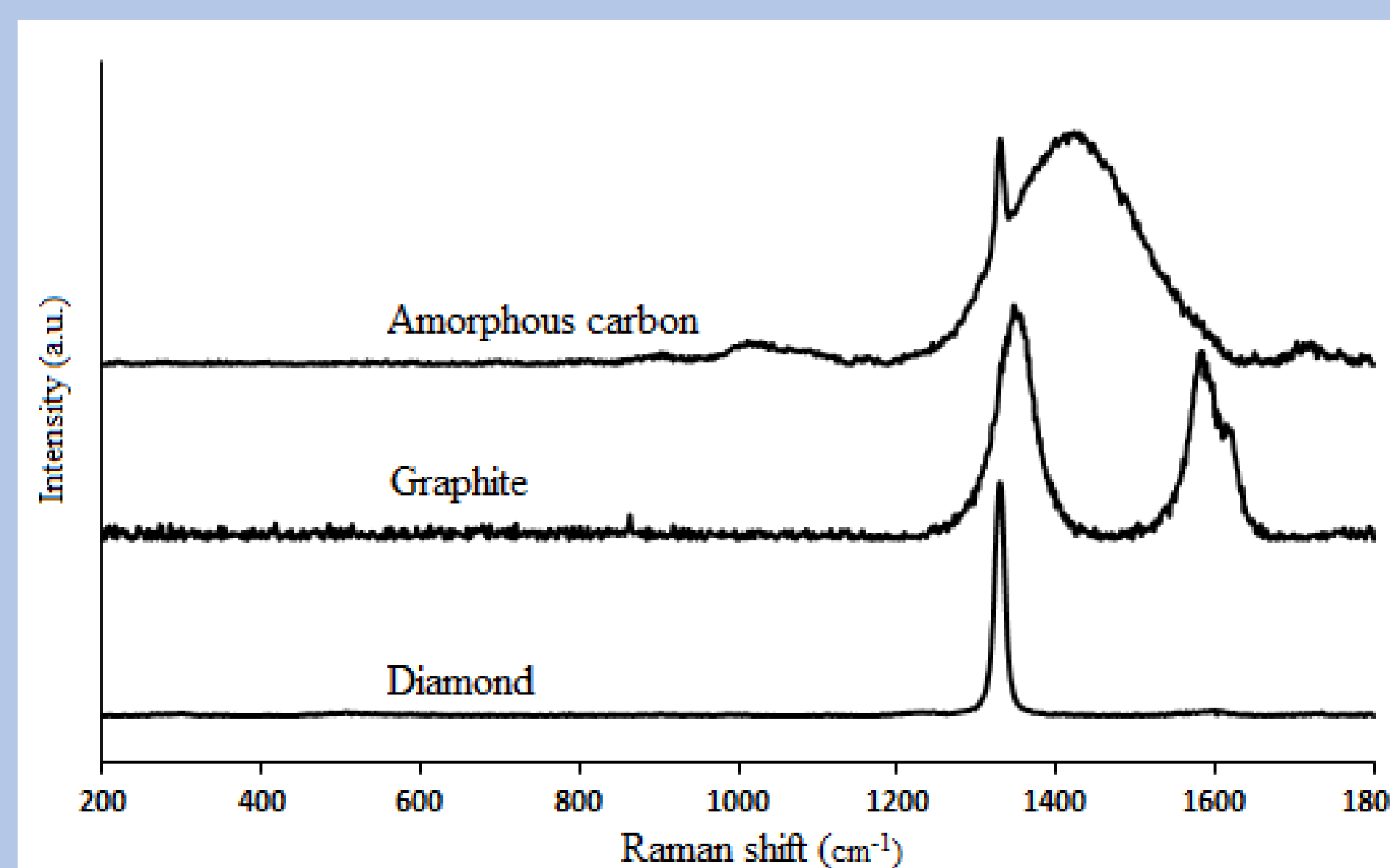


Figure 4: Raman spectra of carbonaceous phases found in Nova 018, with baseline corrections confirming the presence of both diamond and graphite. Analogous to terrestrial samples, diamond spectra are centered at 1331 cm^{-1} . Graphite spectra include both the D and G bands centered at 1348 and 1589 cm^{-1} , respectively [7,12]. Amorphous carbonaceous material have very wide Raman spectra peaks centred around 1440-1470 cm^{-1} and may include the sharp D band [12].

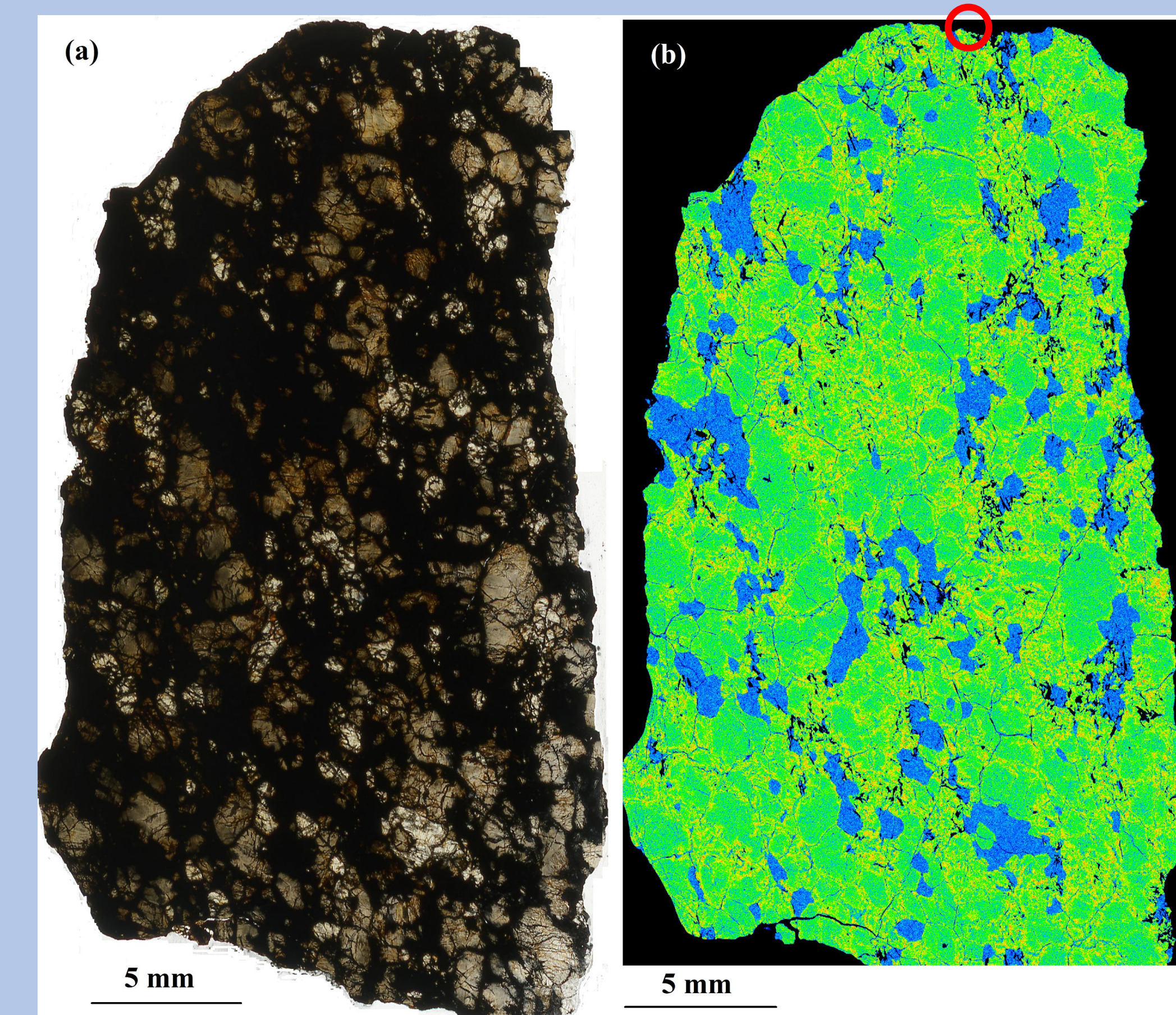


Figure 3: (a) Scanned image of the Nova 018 thin section. (b) Element distribution map of Mg showing different phases: CPX = blue; olivine = green; carbon, sulphides, metal = black; reduction rims = yellow / red.

Raman spectroscopy confirms the presence of both diamond and graphite (**Figure 4**).

- Analogous to terrestrial samples, diamond spectra are centered at 1331 cm^{-1} .
- Graphite spectra include both the D and G bands centered at 1348 and 1589 cm^{-1} , respectively [8,13].
- Amorphous carbonaceous material have very wide Raman spectra peaks centred around 1440-1470 cm^{-1} and may include the sharp D band [13].

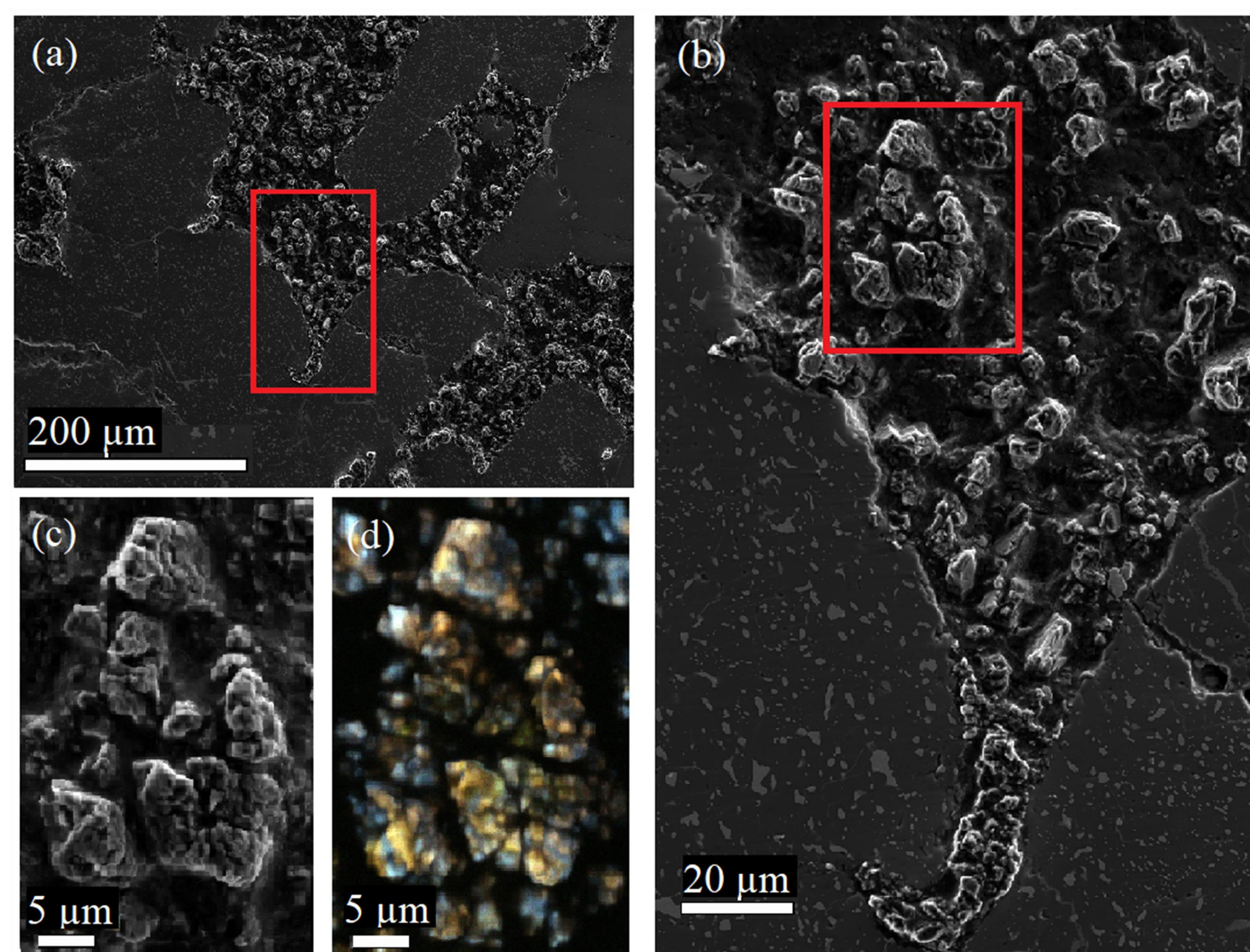


Figure 5: SEM-BSE and CL images of a carbon-rich domain. (a) BSE image of carbon-rich domain. (b) Magnified BSE image of high-relief diamonds. (c) High magnification BSE image of boxed in diamond cluster. (d) colored CL image of diamond cluster in (c) showing chemical zonation.

Nova 018 appears unique by the size and abundance of its diamonds. Research to date suggests ureilitic diamonds in this sample range from nanometers up to tens of microns [12,14,15].

- The exceptional size of Nova 018's microdiamonds could indicate slow growth in the HPHT environment or by CVD in the solar nebula [14].
- It is possible that the coexistence of diamond with graphite could be explained by back transformation from diamond to graphite under heat exposure or by simultaneous growth of graphite as a metastable phase [14].
- The blue and yellow colors produced by CL imaging could indicate growth by CVD and natural polycrystalline diamond, respectively [15].

If the diamonds in Nova 018 are oriented, the HPHT theory would be unable to explain its uniaxial growth [16], however, it could be explained by CVD or a high-impact shock event transforming graphite into diamond [17].

The conflicting data and theories create a complex scenario. Further analysis to determine the nucleation and growth histories of the nano- and micro-diamonds is required. It is possible that the petrogenesis of Nova 018's varied and abundant carbon phases involve a combination of any of these theories.

Future Work

- Abundances of highly siderophile elements will be conducted using either Laser Ablation Inductively Coupled Plasma Mass Spectrometry (LA-ICP-MS) or solution dissolution.
- The total count of diamond abundances will be attempted utilizing either transmitted ultraviolet petrographic microscopy or computed tomography (CT).
- Further analysis to confirm the presence of oriented diamonds is required to better constrain method of formation.

About the author

At the young age of 35, Steve left his career in retail management to pursue a second degree in rocks. He discovered a passion for meteorites during a Special Topics course, taught by Dr. Tait, on Meteorites and Space. Outside of the classroom he cares for his grandmother, 2 dogs and cat. He is an avid world traveller, has a passion for fitness, and loves sushi.



Acknowledgements

Thank you to Dr. D. Gregory who graciously donated this meteorite to the ROM. We appreciate the technical support from Y. Liu (University of Toronto) and I. Barker (Western University) with the EPMA and SEM analyses, respectively. Funding was provided by the National Sciences and Engineering Research Council of Canada (NSERC).

References

- [1] Janots et al. (2011) *MAPS*, 46, 134-148 [2] Day et al. (2017) *GCA*, 198, 379-395. [3] Miyahara et al. (2015) *GCA*, 163, 14-26. [4] Urey (1956) *Astrophysical Journal*, 124, 623-637. [5] Nagashima et al. (2012) *MAPS*, 47, 1728-1737. [6] Goodrich et al. (1987) *GCA*, 51, 2255-2273. [7] Boyle (2017) *Nova 018* [photograph], Royal Ontario Museum, Toronto, Canada. [8] Lafuente et al. (2015) *Highlights in Mineralogical Crystallography*, 1-29. [9] Goodrich et al. (2014) *GCA*, 135, 126-169. [10] Mittiefelid et al. (1998) *Planetary Materials*, 4.1-4.195. [11] Stoffler et al. (1991) *GCA*, 55, 3845-3867. [12] Nakamura et al. (2016) *Journal of Mineralogical & Petrological Sciences*, 111, 252-269. [13] Wopenka et al. (2013) *GCA*, 106, 463-489. [14] Miyahara et al. (2015) *GCA*, 163, 14-26. [15] Karczewska (2010) *Journal of Achievements in Materials and Manufacturing Engineering*, 43, 94-107. [16] Nagashima et al. (2012) *MAPS*, 47, 1728-1737. [17] Matsuda et al. (1991) *GCA*, 55, 2011-2023.